

## RESEARCH ARTICLE

# Validation of Reference Genes for Robust qRT-PCR Gene Expression Analysis in the Rice Blast Fungus *Magnaporthe oryzae*

Sarena Che Omar<sup>1</sup>, Michael A. Bentley<sup>1</sup>, Giulia Morieri<sup>1</sup>, Gail M. Preston<sup>1</sup>, Sarah J. Gurr<sup>1,2\*</sup>

**1** Department of Plant Sciences, University of Oxford, South Parks Road, Oxford, OX1 3RB, United Kingdom, **2** BioSciences, Geoffrey Pope Building, University of Exeter, Exeter, EX4 4QD, United Kingdom

\* [S.J.Gurr@exeter.ac.uk](mailto:S.J.Gurr@exeter.ac.uk)

CrossMark  
click for updates

 OPEN ACCESS

**Citation:** Che Omar S, Bentley MA, Morieri G, Preston GM, Gurr SJ (2016) Validation of Reference Genes for Robust qRT-PCR Gene Expression Analysis in the Rice Blast Fungus *Magnaporthe oryzae*. PLoS ONE 11(8): e0160637. doi:10.1371/journal.pone.0160637

**Editor:** Richard A Wilson, University of Nebraska-Lincoln, UNITED STATES

**Received:** May 3, 2016

**Accepted:** July 23, 2016

**Published:** August 25, 2016

**Copyright:** © 2016 Che Omar et al. This is an open access article distributed under the terms of the [Creative Commons Attribution License](http://creativecommons.org/licenses/by/4.0/), which permits unrestricted use, distribution, and reproduction in any medium, provided the original author and source are credited.

**Data Availability Statement:** All relevant data are within the paper and its Supporting Information files.

**Funding:** We acknowledge funding from Khazanah Foundation in support of SCO, BBSRC grant BB/J008923/1 awarded to SG and we thank Eleanor Jaskowska for her assistance in tissue preparation. Neither funder played a role in study design, data collection, analysis, decision to publish or manuscript preparation.

**Competing Interests:** The authors have declared that no competing interests exist.

## Abstract

The rice blast fungus causes significant annual harvest losses. It also serves as a genetically-tractable model to study fungal ingress. Whilst pathogenicity determinants have been unmasked and changes in global gene expression described, we know little about *Magnaporthe oryzae* cell wall remodelling. Our interests, in wall remodelling genes expressed during infection, vegetative growth and under exogenous wall stress, demand robust choice of reference genes for quantitative Real Time-PCR (qRT-PCR) data normalisation. We describe the expression stability of nine candidate reference genes profiled by qRT-PCR with cDNAs derived during asexual germling development, from sexual stage perithecia and from vegetative mycelium grown under various exogenous stressors. Our Minimum Information for Publication of qRT-PCR Experiments (MIQE) compliant analysis reveals a set of robust reference genes used to track changes in the expression of the cell wall remodelling gene *MGG\_Crh2* (MGG\_00592). We ranked nine candidate reference genes by their expression stability (M) and report the best gene combination needed for reliable gene expression normalisation, when assayed in three tissue groups (Infective, Vegetative, and Global) frequently used in *M. oryzae* expression studies. We found that *MGG\_Actin* (MGG\_03982) and the 40S 27a ribosomal subunit *MGG\_40s* (MGG\_02872) proved to be robust reference genes for the Infection group and *MGG\_40s* and *MGG\_Ef1* (Elongation Factor1- $\alpha$ ) for both Vegetative and Global groups. Using the above validated reference genes, *M. oryzae MGG\_Crh2* expression was found to be significantly ( $p < 0.05$ ) elevated three-fold during vegetative growth as compared with dormant spores and two fold higher under cell wall stress (Congo Red) compared to growth under optimal conditions. We recommend the combinatorial use of two reference genes, belonging to the cytoskeleton and ribosomal synthesis functional groups, *MGG\_Actin*, *MGG\_40s*, *MGG\_S8* (Ribosomal subunit 40S S8) or *MGG\_Ef1*, which demonstrated low M values across heterogeneous tissues. By contrast, metabolic pathway genes *MGG\_Fad* (FAD binding domain-containing protein) and *MGG\_Gapdh* (Glyceraldehyde-3-phosphate dehydrogenase) performed poorly, due to their lack of expression stability across samples.

## Introduction

Rice blast disease is caused by the ascomycete fungus *Magnaporthe oryzae* (previously known as *Magnaporthe grisea* [1]). Despite active pathogen management strategies, such as the deployment of disease resistant cultivars and the widespread spraying of antifungals, year-on-year crop losses occur. Indeed, recent rice blast outbreaks have been seen in USA, Thailand, China, India and Japan [2–5]. With significant annual yield losses (up to 30%) attributable to this fungus alone, and as the global demand for rice increases alongside population growth, better control of this disease is imperative [6–8]. Recent years have seen growing interest in the fungal cell wall as a potential phylum-specific target for disease mitigation. In this regard, our quest is to describe the mechanisms which underpin cell wall construction and which endow it with sufficient plasticity to support expansion, growth and infection [9–11]. To achieve such plasticity, specialised groups of GPI-anchored glycosyltransferase (GST) proteins such as Gasp/Gelp, [12–14], Crh1p/Crh2p [15, 16], Dfg1p/Dcw5p [17] and Sps2p (Ecm33p) [18] continuously remodel synthesised polysaccharides in response to changes in the external environment or with the developmental clock [12, 13, 16, 17]. Of the various GSTs, the *Crh*-like family of Crhp, carrying Crh1p, Utr2p and Crr1p was first described in *Saccharomyces cerevisiae* [19]. These proteins share a functional domain belonging to the Glycosyl Hydrolase 16 group of Carbohydrate Active Enzymes (CaZy) and catalyse the hydrolysis of  $\beta$ -(1,4) linkages in the chitin polymer and the transfer of chitin to a glucan acceptor, usually to either  $\beta$ -(1,3) or (1,6) glucan chains, and subsequent branch formation with chitin polymers [20, 21]. The cross-linking of these alkaline-insoluble chitin chains to the soluble glucan polymers is responsible for providing cell wall rigidity and strength [22, 23] and therefore inactivation of the *Crh*-like proteins could potentially influence fungal pathogenicity. In agreement with this, *Candida albicans* knockout mutant strain  $\Delta$ Utr2 was less virulent and unable to colonize mice organs [24]. Furthermore, Pardini et al. [15] then developed a triple mutant which was fully non-pathogenic even when mice were infected at a lethal dose. Results from the studies above are an important indication that targeting *Crh*-like genes has the potential to impair a pathogen's viability, subsequently affecting its ability to infect and/or colonize a host.

Little is known about this family of genes in plant pathogenic fungi. As a first step, we set out to capture the expression profile of *M. oryzae* MGG\_Crh2 (orthologous to *Crh1* in *S. cerevisiae*) during fungal development (asexual morphogenesis, sexual structure formation and vegetative growth) and when grown under cell wall stress (Congo Red). This undertaking posed several technical challenges, not least the paucity of pathogen RNA present within the host tissues (often <0.1%). In *S. cerevisiae*, temporal expression of *Crh1* increases by 2-fold as the yeast enters the budding phase, whilst under cell wall stress, invoked by Congo Red, Calcofluor White or Zymolyase, expression increases by 2–4 fold [25, 26]. Despite these small fold changes, yeast *Crh* mutants exhibit hypersensitivity to these cell wall perturbing compounds, as well as altered cell surface plasticity [22]. Such small fold changes in protein transcript abundance further re-enforce the need for a sensitive, reliable and robust quantification technique.

A multitude of publications attest to the usefulness of both individual and genome-wide gene expression studies in *M. oryzae*. However, whilst large-scale transcript analyses with microarrays and/or high throughput-SUPERSAGE have captured gross fold-changes over several thousand genes [27, 28], such analyses are not sensitive enough to detect small changes in low abundance genes. Moreover, they are overly challenging or, indeed, impossible to perform with minute samples of tissue-specific RNA. Quantitative Real-Time PCR provides a low throughput (*ie* a restricted number of genes) but highly sensitive technique [29, 30]. Indeed, it has been shown to be 5-fold more sensitive than microarray data [31]. However, to obtain reliable data, qRT-PCR requires stringent preparation strategies, including good quality RNA

samples and the use of efficient and specific primers [32–34]. In addition, the choice and number of reference genes used for data normalisation are critical for robust analysis of gene expression [34, 35]. Studies have shown that expression stability of a reference gene varies between species, and that expression could also vary across sample tissue type and experimental conditions [32, 33, 36, 37]. Moreover, using an inappropriate number of reference genes can adversely affect data reliability—as shown with *Drosophila melanogaster* head cDNA, where the relative expression of genes *GSTDI*, *INR* and *HSP70* differed significantly when the normalising factor (NF) used either 1, 3 or 13 reference genes [38]. As such, the use of un-validated and/or single reference genes in qRT-PCR assays, such as, for example, *MGG\_β-Tubulin*, *MGG\_Actin*, *MGG\_Gapdh* or *MGG\_Ubiq* in *M. oryzae* is strongly discouraged. In addition, sample quality control, validation, and assay optimisation prior to running the qRT-PCR in gene expression assays are important for data reliability. Recognising this, recently there has been an increase in the number of reference gene validation studies in plant fungal pathogens such as in *Puccinia* sp. (wheat rust) [39], *Fusarium* sp. (wheat head blight) [40], and *Aspergillus* sp. (Black mould) [41]. However, prior to the work conducted by Park et al. [27], studies of gene expression in *M. oryzae* used only one, un-validated reference gene such as *MGG\_β-Tubulin* [42, 43], *MGG\_Actin*, or *MGG\_Gapdh* [44]. To redress this, Park et al. [27] recently attempted to validate seven candidate genes, identifying *MGG\_β-Tubulin* as the most stably-expressed gene of their cohort. The work, however, comes short of identifying the appropriate number of reference genes to use.

Through the emphasis for stringent qRT-PCR preparation, this paper was prepared in accordance to the guidelines made for the Minimum Information for Publication of qRT-PCR Experiments (MIQE) [34]. Furthermore, given the need to improve current measurement of gene expression practices in *M. oryzae* studies, this paper utilises additional candidate reference genes as well as genes commonly used in this field of study. Here, nine candidate reference genes from various functional groups were shortlisted, the stability validated and importantly, the appropriate number of genes needed for normalisation of gene expression under various fungal growth conditions were determined in this study. We then used the chosen reference genes to investigate the expression profile of *MGG\_Crh2*, a cell wall remodelling protein, during various developmental stages and growth under various exogenous stresses. Thus, we have evaluated and determined the optimal number of reference genes to use, but have also appraised and added several further candidate genes, from disparate functional groups that out-perform the expression stability of *MGG\_β-Tubulin* as the ideal reference gene. We hereby propose a robust qRT-PCR data normalisation strategy for transcript analysis in *M. oryzae* that will improve the confidence and reliability of all future gene expression analysis work related to this fungus.

## Materials and Methods

### Fungal Strains and Growth Conditions

Rice blast fungus *Magnaporthe oryzae* (*M. grisea* (T.T. Herbert) M.E. Barr) wild type (WT) strains Guy11 (MAT1-2) and TH3 (MAT1-1) were cultured on complete medium (CM) at 24°C, 14 hour light 10 hour dark cycle. Strain maintenance and media composition were as described by Talbot et al. [45]. Perithecia were produced by crossing Guy 11 with the opposite mating type strain TH3: agar plug inocula of the 2 strains were placed 4 cm apart on oatmeal agar and incubated under constant fluorescent light at 18°C for 29 days. Perithecia were then harvested using a dissecting microscope and snap-frozen in liquid nitrogen. Guy11 spores were harvested from 10-day-old CM plates by scraping the surface with 10 mL deionised water with a glass slide, and poured through triple layered Miracloth (Merck Chemicals Ltd, Padge Rd,

Nottingham, NG9 2JR, UK). Spore concentrations were adjusted using a haemocytometer prior to use.

## Tissue Preparation for RNA Extraction

**Mycelial tissue grown under various stress factors.** Two hundred  $\mu\text{L}$  of  $4 \times 10^5$  spores/mL Guy11 spore suspension was added to 500 mL of various liquid cultures, and incubated at  $24^\circ\text{C}$  for 3 days in the dark, under continuous shaking (150 rpm). Mycelia were harvested by filtering through double-layered Mira-cloth, dried with paper towels and 0.1 g of fungal mycelia was snap frozen in liquid nitrogen and stored at  $-80^\circ\text{C}$ . The process was repeated to gather three biological replicate samples for each condition assayed.

For control vegetative growth under optimal conditions, *M. oryzae* Guy11 was cultured in Complete Medium (CM). Starvation was achieved by culturing in Minimal Medium (MM) made from 1x nitrate salts, 1% D-glucose, 0.1% ml trace elements solution, 0.1% thiamine solution, and 0.05% biotin solution. In extreme starvation, glucose was omitted from the Minimal Medium preparation above (MM-glucose). For cell wall stress, the cell wall perturbant Congo Red (SIGMA-Aldrich) was prepared in a 1% stock solution, filter-sterilised and added to sterile Complete Medium buffered with 50 mM HEPES (pH 7.0) at a concentration of 100  $\mu\text{g}/\text{mL}$ . Stress by caffeine was induced by adding 2.5 mM filter-sterilised caffeine (SIGMA-Aldrich) to sterile Complete Medium (pH 6.5). To impose osmotic stress, 1 M Sorbitol was added to Complete Medium (pH 6.5) prior to autoclaving.

**Dormant spores at 0 hours post inoculation (hpi).** Spores were harvested from 10-day-old WT strain Guy11 grown on Complete Medium agar plates, 25 plates per biological replicate (three biological replicates harvested separately). The combined spores were centrifuged (5 minutes at 13,000 rpm,  $4^\circ\text{C}$ ), the supernatant removed and the pellet snap frozen in liquid nitrogen.

**Germling development at 2, 8, 24, and 48 hours post inoculation (hpi) on host.** Barley seeds (*Hordeum vulgare* L.) cv. Golden Promise were grown in a 50:50 (w/w) mixture of Erin Multipurpose Compost and John Innes No. 2 soil-based compost, for 7 days at  $25^\circ\text{C}$ , 12/12 light, 70% humidity. Seven-day-old barley leaves were cut and placed onto 1.5% (w/v) water agar and inoculated with harvested spores ( $6\text{--}7 \times 10^6$  spores/mL) re-suspended in 0.4% (w/v) gelatine. Inoculation procedure: for each time point, 2.5 mL of the spore suspension was sprayed uniformly onto 24 leaves, which were then covered to maintain high humidity and incubated at  $25^\circ\text{C}$  for 2, 8, 24 or 48 hours post inoculation. The hours post inoculation (hpi) corresponds to the various infective stages: 2 hpi (germ tube emergence), 8 hpi (immature appressoria), 24 hpi (penetration and early invasive growth), and 48 hpi (*in planta* growth). Prior to harvest, one leaf was selected at random, and its surface viewed by light microscopy to monitor germling development and formation of appressoria. Approximately 0.1 g of leaf material was then snap frozen in liquid nitrogen and stored at  $-80^\circ\text{C}$ , for RNA extraction. The process was repeated, harvesting three biological replicates.

**Perithecia.** Guy11 and TH3 were inoculated onto oatmeal (10% (w/v)) agar and incubated as described previously. Perithecia (0.1 g) were harvested, snap frozen in liquid nitrogen and kept stored at  $-80^\circ\text{C}$  prior to RNA extraction. Three biological replicates were harvested independently.

## RNA Extraction, Quantity, and Quality Test

Tissues were extracted with TRIzol<sup>®</sup> Reagent (Ambion<sup>®</sup>) using the manufacturers' instructions, followed by the addition of 50% volume isopropanol, with 5 minutes incubation at room temperature. Samples were loaded into an RNA Quick Spin column (Qiagen RNeasy Minikit)

for on-column DNase digestion and subsequent elution in RNase-free water. RNA sample concentration was determined using the Thermo Scientific 'NanoDrop® ND-1000' spectrophotometer. Samples were normalized to the same concentration of 1000 ng/μL (±100 ng). RNA quality and RIN number for each sample were tested using the 'Agilent 2100 Bioanalyzer Instrument' as per the manufacturers' instructions to ensure minimal RNA degradation. Sample RNA was discarded if the RIN value was below 7.5 for samples containing only fungal RNA, and if the RIN value was below 6.0 for samples containing a mix of plant leaf and fungal pathogen RNA.

### cDNA Preparation

Qiagen 'Maxima First Strand cDNA Synthesis Kit for RT-qPCR' kit was used as per manufacturers' instructions. The same amount of template RNA (1.0 μg), was added per 20 μl reactions for each tissue sample. Three controls were prepared: Non-template control (NTC), minus Reverse Transcriptase (-RT) and RNA from Barley leaf only (BL). The reaction mix was incubated for 10 min at 25°C, followed by 30 min at 50°C, and the reaction terminated by heating at 85°C for 5 min. Products were retained at -20°C and used within 2 weeks.

### Candidate Reference Gene Selection and Primer Design

Candidate reference genes were selected on the basis of being (a) previously used in *M. oryzae* gene expression studies [42, 43, 46–48], and (b) from several essential functional groups (protein translation, glycolysis pathway, cytoskeleton). These genes were then cross-checked with the publicly available COGEME high throughput-super SAGE transcript profile *M. oryzae* database [49], for an estimation of stability. Stability ratios were calculated using the given base mean values between samples of the same growth stage (example: Complete Medium against Minimal Medium, or 4 hpi against 16 hpi). Genes with a ratio less than 10 from the transcriptomic database were then selected for further analysis. Sequences for the respective genes were obtained from the 8<sup>th</sup> annotation (MG8) *Magnaporthe oryzae* strain 70–15 sequenced by Broad Institute [30]. All primer pairs (Table 1) were synthesized by SIGMA-Aldrich and designed according to the following specifications: annealing Tm 60°C (±2°C); G-C content 50–60%; no non-specific product amplification; no primer-dimer or secondary structures; amplicon of 60–110 bp; primer efficiency 80–110%, r<sup>2</sup> value 0.98–0.99; either Forward or Reverse primer to span exon/exon boundary (transcript-specific). Primer specificity: primers were deemed acceptable if the targeted gene showed an e value less of than 10<sup>-3</sup> in NCBI Blast search. In addition, primer pairs were shown to be pathogen-specific by conducting qRT-PCR using only host barley leaf cDNA as a negative control (BL). Primers were tested for non-specific product/s by amplicon separation on 2% (w/v) agarose gel electrophoresis and 10–300 bp GeneRuler Ultra Low Range DNA Ladder (Thermo Scientific) at the end of a qRT-PCR run. [50]

### Quantitative Real Time PCR (qRT-PCR)

Real time PCR for the Infective group was conducted using an Mx3000P qPCR System (Agilent Technologies), which was replaced with an ABI 7000 apparatus (Applied Biosystems) for the Vegetative and Global group. All reactions were conducted in 96-well plates (MicroAmp® Optical 96-Well Reaction Plate cat N8010560) utilising a sample maximisation arrangement and the addition of inter-run calibration (IRC) wells for each gene in each 96-well plate [51]. 'Power SYBR Green PCR Master Mix' assay (Applied Biosystems) was used in a total volume of 25 μL per well/reaction. Each 25 μL reaction contained 2.0 μL cDNA, 8.5 μL water, 1.0 μL (10 μM) forward primer, 1.0 μL (10 μM) reverse primer and 12.5 μL 'Power SYBR Green PCR

**Table 1. Information regarding genes used and primers designed for this study.**

Gene name	Gene ID and accession num	Symbol used	Forward Primer*	Reverse Primer*	Size (bp)	Efficiency (E)	R <sup>2</sup> Value	Reference
β-Tubulin chain	MGG_00604 (XM_003718381)	MGG_β-Tubulin	CTGCCATCTCCGTGGAAGG	GACCAAGTACGACGAGTTCTTG	86	1.95	0.9998	[50]
Elongation factor 1-α	MGG_03641 (XM_003716200)	MGG_Ef1	CATCTTAAAGTCGTCGTCATC	AGTGGCCGGTAGTCGTGG	62	1.92	0.9995	This study
Actin	MGG_03982 (XM_003719823)	MGG_Actin	ACAATGGTTCCGGTATGTGC	CGACAATGGACGGGAAGAC	76	2.02	0.9975	This study
Ubiquitin-conjugating enzyme	MGG_04081 (XM_003719709)	MGG_Ubiquitin	ATCCTAATGTCTACCCGAG	GATGCGTGTTCGTAGTGG	85	1.99	0.9996	This study
Glyceraldehyde-3-phosphate dehydrogenase	MGG_01084 (XM_003717805)	MGG_Gapdh	CAAGTACGCCCAAAATACATGC	TTGCCGTTGACGACCAGG	96	2.06	0.9988	This study
40S ribosomal protein subunit S27a	MGG_02872 (XM_003720814)	MGG_40S	ACAAGCTCAAGACCCCTCGTC	GGTGGTATGGTGAAGCAG	80	1.95	0.9996	This study
40S ribosomal protein subunit S8	MGG_03251 (XM_003716675)	MGG_S8	GCTCACTACCCCCAGAAGC	ACGGACGGTGTGAATCGG	87	1.90	0.9989	This study
FAD binding domain-containing protein	MGG_01605 (XM_003714541)	MGG_Fad	ACCTTGTGGCTGGGATG	TCCATCGAGTACACCCAC	104	2.04	0.9984	This study
Nucleolar Protein	MGG_07008 (XM_003709718)	MGG_Nuc	AGTGGGGTTATGGTCTCTTC	CTGCTCTCCAGGTCATCTGC	64	2.04	0.9978	This study
Crh2 cell wall <i>glycosyltransferase</i> gene	MGG_00592 (XM_003718400)	MGG_Crh2	GAGATCGACTGGGAGCACG	AGACGGTGTCAITACCCTTGG	79	1.98	0.9955	This study

\*underlined nucleotides represent the second exon in a primer that anneals to an exon/exon boundary

doi:10.1371/journal.pone.0160637.t001



Master Mix'. All qRT-PCR plate amplifications followed the thermal cycler steps: 50°C for 2 minutes followed by 95°C for 10 minutes; 95°C 15 seconds, followed by 60°C annealing temperature for 1 minute, repeating this final step for 40 cycles. Fluorescence of the 'SYBR Green I' dye was calibrated against ROX™. At the end of each reaction, a dissociation curve analysis was performed, with the following thermal profile: 95°C for 15 seconds; 60°C for 30 seconds followed by 95°C for 15 seconds. Data from each group of tissue type (Infective, Vegetative, and Global) was analysed independently (both geNorm and expression profile).

### Primer Efficiency, Specificity, and Genomic DNA Contamination Check

Complementary DNA (cDNA) from all samples was pooled, diluted 5-fold and used as templates. Cycle threshold (Ct) values were analysed as follows: the primer efficiency (E) was calculated from the four point slope of the plotted dilution row, using the formula  $E = 5^{(1/S)}$  whereby S is the slope of the regression line. Primer pairs with slope  $r^2 < 0.99$ ,  $E < 1.8$  or dissociation curve and gel electrophoresis runs showing non-specific product/s, were rejected and re-designed, prior to gene stability analysis. Primer efficiency data is shown in [Table 1](#). For further quality control purposes, samples with technical replicates showing more than 0.8 difference in Ct value, or occurrence of amplification in non-template and host-only control (BL) with Ct values less than 35, were rejected.

### Evaluation of Reference Gene Expression Stability Using GeNorm Analysis

Analysis of raw Ct data for all candidate reference genes was performed using 'qBase+ Basic' licensed software (Biogazelle). Each group (Infective, Vegetative, and Global) was analysed separately. The Infective group included tissues from dormant spores (0 hpi) and at various time points corresponding to different *M. oryzae* infective stages: germ tube (2 hpi), immature appressoria (8 hpi), mature appressoria (12 hpi), penetration peg and haustoria (24 hpi), and extensive *in planta* growth (48 hpi). The Vegetative group included vegetative stage fungal mycelia harvested from an optimal growth condition (CM) and under various environmental stresses such as starvation (MM), extreme starvation (MM-glucose), osmotic stress (Sorbitol), cell wall stress (Congo Red) and caffeine stress. The Global group included a mixture of the above: dormant spores, immature appressoria (8 hpi), CM, starvation (MM) and perithecia (sexual reproductive stage).

For each group (Infective, Vegetative or Global), raw ct values were converted to relative expression values using the Pfaffl Method [52] and inter-run calibration was performed to correct for run-to-run variation [51]. The GeNorm algorithm [53] in 'qBase+ Basic' licence software version 2.5 (Biogazelle) was used to calculate the average expression stability score (M) for each reference gene, and the pairwise variability score (V) for sequential normalisation factors, resulting from stepwise inclusion of additional reference genes. Expression stability values were used to identify the most stably-expressed reference genes at each stage, whilst pairwise variability scores were used to determine the most appropriate number of reference genes to use as the normalisation factor.

### Gene of Interest (GOI): Orthologue of *S. cerevisiae* *Crh1* gene

The *Crh1* gene was first identified in the model yeast *S. cerevisiae* [19]. The protein sequence was obtained from the Saccharomyces Genome Database [54] and the corresponding orthologue in *M. oryzae* was obtained from "Magnaporthe comparative Sequencing Project" by the Broad Institute of Harvard and MIT [30] using the BLASTp search tool [55]. Here, the yeast *Crh1* protein sequence was queried against proteins predicted to be encoded by the *M. oryzae* 70–15 (MG8)

sequenced genome. The best hit genes with a cut-off value of  $e^{-10}$ , were then reciprocal BLASTp [55] against *S. cerevisiae* genome in the NCBI database ([www.ncbi.nlm.nih.gov](http://www.ncbi.nlm.nih.gov)).

### Data analysis: Expression Profile of *MGG\_Crh2* Across the *M. oryzae* life-cycle

The validated combination of reference genes according to tissue types were used as Normalising Factor (NF) to analyse the expression profile of a cell wall remodelling enzyme, *MGG\_Crh2* (MGG\_00592) under various stages of the life cycle (Infective and Global assay) and growth conditions (Vegetative assay). In the latter, the expression of *MGG\_Crh2* under starvation (MM), osmotic stress (Sorbitol), extreme starvation (MM-glucose), and cell wall stress imposed by Congo Red (CR) or caffeine was measured relative to vegetative growth in nutrient-rich medium (CM). In the Infective assay, expression profile was measured during germling development for tissues harvested from 2 hpi (germ tube), 8 hpi (immature appressoria), 24 hpi (penetration and early invasive growth) and 48 hpi (*in planta* growth), relative to 0 hpi (dormant spores). Finally, the expression profile of *MGG\_Crh2* was captured across all stages of the life cycle in the Global assay by comparing *MGG\_Crh2* expression in representative tissues. These were 8 hpi (immature appressoria), 48 hpi (*in planta* growth), vegetative growth (CM) and perithecia, relative to 0 hpi (dormant spores).

Two technical replicates were used per reaction. When possible, the plate design carried all three biological replicates for target and control sample respectively, on the same plate; and, for each sample analysed, *MGG\_Crh2* and two validated reference genes were deposited onto the same plate. For expression analysis involving more than one 96-well plate, comparison of samples across different plates was achieved by incorporating inter-run calibration (IRC) wells for each gene in equivalent wells within each 96-well plate. The generated Ct values for samples from multiple runs were imported into MxPro QPCR Software or 'qBase-Plus Basic Version 2.5' for IRC calibration [51].

The calibrated values from multiple runs and raw Ct values from one well, were exported into a Microsoft Excel file and analysed separately according to the recommendations by Williams et al. (56). In particular, following their protocol we log transformed, mean centered, and autoscaled the data from three biological replicates, before evaluating the significance of up/down regulation at the 0.05 level by observing whether or not the 95% confidence interval for fold-change increase/decrease in expression contained a fold-change value of 1 (no change). Significant up/down regulated results are indicated by an asterisk on all graphs.

## Results & Discussion

Nine candidate reference genes (Table 1) were selected on the basis of being (a) previously used in *M. oryzae* gene expression studies [42, 46, 47], (b) from several essential functional groups (protein translation, glycolysis pathway, cytoskeleton) and (c) expression data in the publicly available high throughput-superSAGE transcript profiling COGEME database of *M. oryzae* [49]. A base mean ratio above 10 in the COGEME database was interpreted as indicating that gene expression was unstable, and the gene was unsuitable to be a candidate reference gene. Genes with a base mean ratio below 10 were selected for subsequent sensitive analysis (qRT-PCR using GeNorm calculations) to identify the most stable gene.

### Primer Specificity and Efficiency Check

Each primer specificity assay yielded a single amplicon of the expected size for the primer sets tested (Table 1 and S1 Fig–S2 Fig). There was no amplification, or high Ct values (>35 Ct), for both non-template controls, minus reverse transcriptase (-RT) and the host-only control (BL).



This showed that the reagents were free from contamination as there was no amplification of gDNA and no non-specific amplification of plant cDNA. Calculation of primer efficiencies using five-fold dilution of pooled complementary DNA (cDNA) for all nine HKG primers and *MGG\_Crh2* gave  $r^2 > 0.99$  and 80–110% efficiency (E) values (S3 Fig).

## RNA and cDNA Quality and Quantity Check

The RNA Integrity Number (RIN) values derived from pure fungal RNA samples (dormant spores, perithecia, and vegetatively-grown tissues) were  $>7.5$  (S4 Fig), whilst those containing a mix of pathogen and host plant tissues had RIN values  $>6.0$  (S5 Fig). The lowered RIN values from plant-derived RNA were attributable to the presence of both pathogen and host leaf RNA (contributing cytosolic and chloroplastic ribosomal RNA), giving rise to additional multiple peaks during electrophoretic separation. Consequently, the slightly lowered RIN number is not due to actual nucleic acid degradation (RIN  $<6.0$ ), but due to the presence of additional peaks, which increases the calculated total area below the electrophoretic graph, a measurement required for the RIN algorithm [56, 57].

## Expression Stability of Candidate Reference Genes

The gene stability (M) values of the nine candidate reference genes, assayed separately for each group of tissues (Vegetative, Infective, and Global), are shown in Fig 1. Candidate genes with the lowest M value were the most stably expressed, whilst genes with the highest M value were least stable. The minimum number of reference genes required for reliable and accurate normalisation for each tissue group was determined as two genes, with a “cut-off” value was set at 0.15 [53] as shown in Fig 2. The gene stability (M) and pairwise variation (V) measurement data were used to identify the two best-performing reference genes for each group; *MGG\_Ef1* and *MGG\_40s* for the Vegetative Group; *MGG\_40s* and *MGG\_Actin* for the Infection Group, and *MGG\_Ef1* with *MGG\_S8* or *MGG\_40s* (same M value) for the Global Group.

## Reference Gene Validation

Our recommendations for use of the named reference genes for the given tissues are robust but we advocate caution in extrapolation to untested experimental conditions, such as in the use of different exogenous stresses (eg. temperature, pH or heavy metal stress). Moreover, inferred co-regulation is an important consideration in the choice of reference genes and should be avoided, if possible. Here, we selected at least two candidate genes from key functional classes, that is, the glycolysis pathway (*MGG\_Fad* & *MGG\_Gapdh*), protein synthesis (*MGG\_Ef1*, *MGG\_S8* & *MGG\_40s*), cytoskeleton assembly (*MGG\_β-Tubulin* & *MGG\_Actin*) and protein degradation (*MGG\_Ubiq*). For the Infective Group, the two most stable genes, *MGG\_40s*, and *MGG\_Actin* belong to two distinct functional groups. However, for the Vegetative and Global Groups, genes belonging to the protein synthesis pathway proved most robust in stability, being unaffected by changes to environmental stressors or fungal growth phases. In this case, it is more important to use a set of validated stable genes instead of prioritising genes from different biological pathways. Furthermore, for the Vegetative Group, the two most stable genes belong to protein synthesis pathways with exclusive functions: *MGG\_Ef1* and *MGG\_40s*, therefore have little risk of co-regulation [58, 59]. In the Global Group, the most stable genes lie in the protein synthesis pathway. Here, as *MGG\_40s* and *MGG\_S8* both form one 40S functional subunit, we recommend instead *MGG\_Ef1* (M = 0.38), used in conjunction with *MGG\_40s* (M = 0.37) or *MGG\_S8* (M = 0.37). Here, the M value differences are very small, suggesting that all three genes are similarly stable and thus this will not significantly affect normalisation reliability.

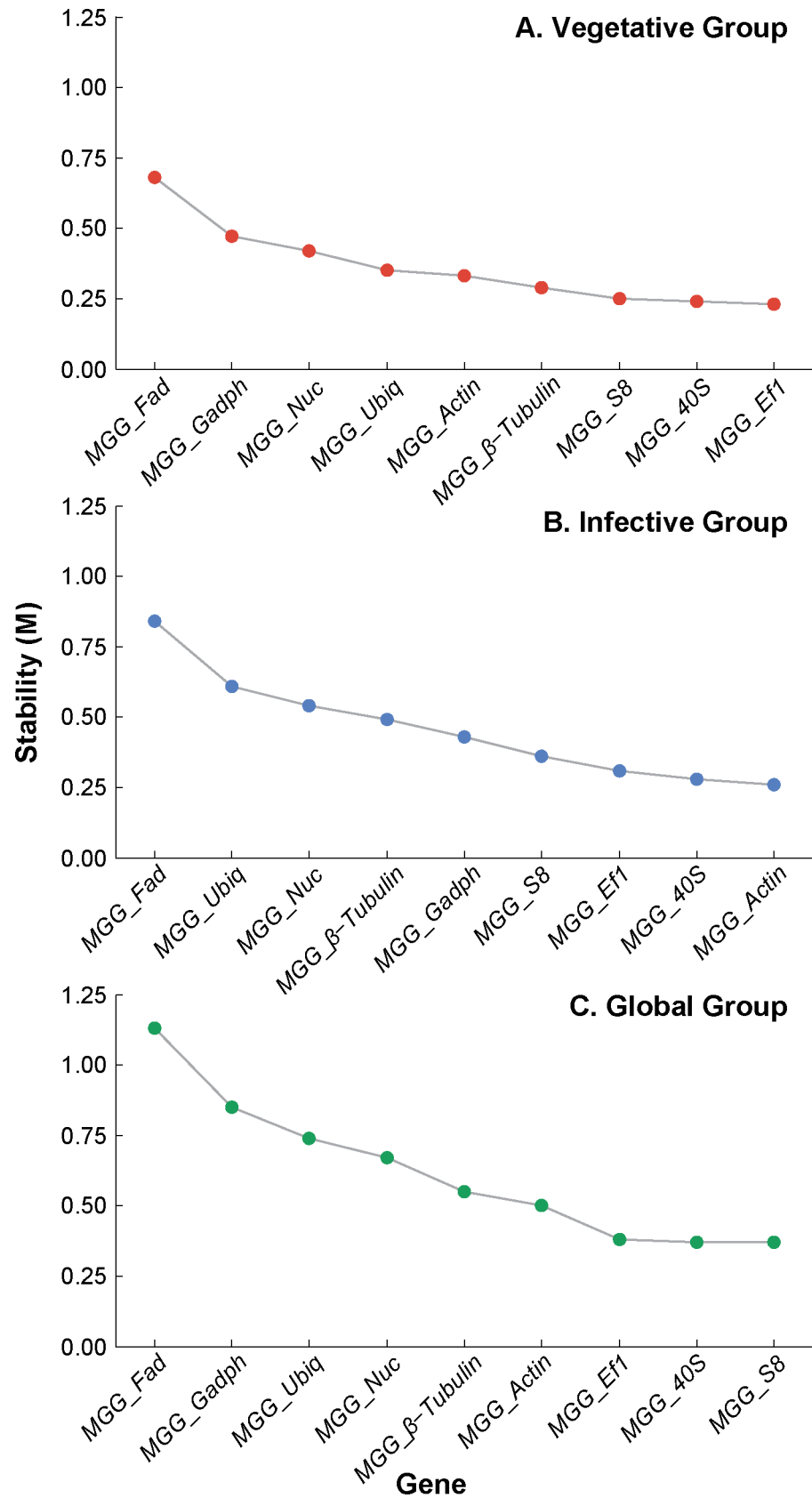


**Fig 1. Ranking of nine candidate reference genes in *M. oryzae* according to the calculated average expression stability (M).** Sequential removal of the least stable reference gene improves average expression stability, indicated by lower values of M. The cut-off for an unstable gene was taken to be  $M \geq 1$ . The analysis was repeated for three groups of tissues: A) Gene stability (M) values for genes in the Vegetative group; B) Gene stability (M) values for genes in the Infective group and; C) Gene stability (M) values for genes in the Global group.

doi:10.1371/journal.pone.0160637.g001

Thus far, a single study has attempted identification and validation of *M. oryzae* reference genes for qRT-PCR [27]. In that study, Park et al. (2013) chose seven candidate genes, three of which are used herein and can therefore be compared directly, namely *MGG\_β-Tubulin*, *MGG\_Actin* and *MGG\_Gapdh*. Based on GeNorm analysis, Park et al. (2013) ranked their seven genes across tissue sample types that concur with our Global Group, whereby *MGG\_Gapdh* has lower stability (high M value), with *MGG\_Actin* and *MGG\_β-Tubulin* being more stably expressed (low M value). Our combined findings also correspond for the Infective Group, whereby *MGG\_Actin* is more stable than *MGG\_Gapdh* and *MGG\_β-tubulin*. This consistency between studies confirms the reproducibility and reliability of qRT-PCR when quality control practices were adhered to. In addition to the three genes shared by both studies, here we introduce a validated set of more robust genes, particularly those belonging to the protein synthesis pathway (*MGG\_Ef1*, *MGG\_40s*, and *MGG\_S8*) that can be used for gene expression studies in *M. oryzae*. This study also demonstrates that for accurate and reliable normalisation of *M. oryzae* genes across all tissue groups (Infective, Vegetative, and Global), the optimal

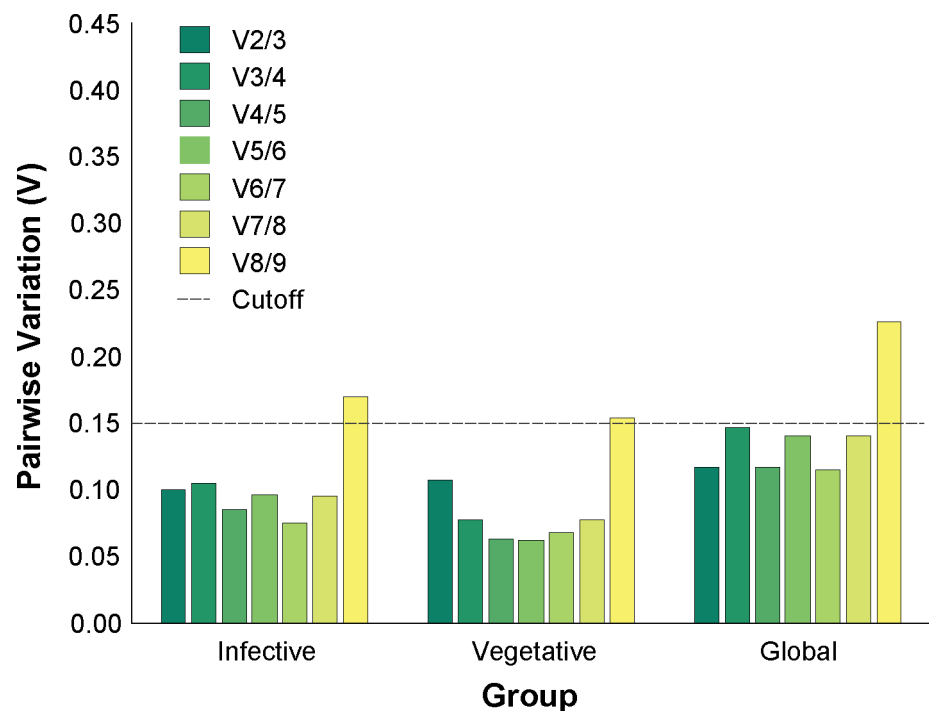


**Fig 2. Determination of the optimal number of reference genes for accurate normalisation.** Graphs show calculated pairwise variation,  $V_{n/(n+1)}$ , between normalisation factor  $NF_n$  and  $NF_{n+1}$  for a total of nine candidate reference genes. The optimal number of reference genes for accurate normalisation was taken to be the smallest number for which V was less than a cut-off of 0.15 [53]. The analysis was repeated for the three designated groups: A) Infective; B) Vegetative, and; C) Global.

doi:10.1371/journal.pone.0160637.g002

number of reference genes to use is two and not one as used in many *M. oryzae* gene expression analysis studies hitherto.

### Gene of Interest (GOI): *MGG\_Crh2* Expression Profile

Reciprocal blast search using the *S. cerevisiae* gene *Crh1* protein sequence revealed *MGG\_00592* as the best-hit gene and most probable orthologue, with a cut-off value of  $e^{-10}$ . It is hereby named *MGG\_Crh2*. We exploited the stable pairs of recommended reference genes as normalising factors to trace the expression profile of the cell wall remodelling gene *MGG\_Crh2*, an orthologue of *S. cerevisiae* *Crh1* gene (S1 Dataset). In the vegetative assay, we used *MGG\_40s* and *MGG\_Ef1* as reference genes and observed that *MGG\_Crh2* expression responded to cell wall stress imposed by Congo Red, being elevated some 2-fold ( $p < 0.05$ ), and was downregulated under extreme starvation (MM-glucose) (Fig 3, Graph A and B) but was not affected by growth under cell wall stress imposed by caffeine, hyperosmotic stress (Sorbitol), or by moderate starvation (MM).

In *S. cerevisiae*, *Crh1* has previously been reported to be upregulated 2–4 fold in the presence of Congo Red [26], and cell wall stress caused by Congo Red was shown to activate the cell wall integrity pathway directly via the phosphorylation of Rlm1 [26]. Additionally, the lack of response to cell wall stress induced by caffeine is an interesting observation. Caffeine is a compound known to activate the cell wall integrity pathway leading to phosphorylation of the *S. cerevisiae* Mpk1 and shown to alter yeast cell wall architecture upon transient exposure to caffeine [60]. Further studies need to be conducted to investigate whether MoMig1p [61], an orthologue of *S. cerevisiae* Rlm1p, indeed regulates the expression of *MGG\_Crh2* under cell wall stress and if so, whether it is selective to certain types of stressors.

In the infective assay, *MGG\_40s* and *MGG\_Actin* were used as the normalising factor with expressions measured relative to 0 hpi (dormant spores). Results in Fig 3 (Graph C) showed that *MGG\_Crh2* is not regulated during germling development as its expression in each tissue type (germ tube, immature appressorium, penetration and early invasive growth as well as *in planta* growth) was not significantly different from dormant spores. This is an interesting outcome, given that in other *M. oryzae* cell wall protein studies cell wall biosynthesis and remodelling enzymes such as the chitin synthase *Chs7* gene [62] and two *Gel* orthologues (*MGG\_11861* and *MGG\_08370*) [63] were found to be upregulated during appressorium development and for the former, mutants were non-pathogenic. Interestingly, studies of the human fungal pathogens *Candida albicans* and *Aspergillus fumigatus* showed that the orthologues of *S. cerevisiae* *Crh1p* (*Crh11p* and *Crf1p* respectively) are specifically detected by the mammalian host immune response system [64–67]. It is therefore conceivable that the lack of upregulation of *MGG\_Crh2* in infective structures aids *M. oryzae* in evading detection. The literature is currently devoid of information on plant immune responses elicited by recognition of secreted fungal cell wall remodelling enzymes. There is however, evidence showing that the cell wall of *M. oryzae* is remodelled during infection to ‘mask’ the fungi with  $\alpha$ -1,3 glucan [68], suggesting that the fungi is indeed under selection to evade detection. This unexplored area of plant-pathogen interactions is worth exploring in future work.

The theory is further supported by results in the Global assay (Fig 3 graph D). In this assay, *MGG\_Crh2* gene expression in tissues representative of each stage of the life cycle was each measured relative to dormant spores (0 hpi). Data analysis showed that this gene is most highly expressed during vegetative growth by up to 3-fold higher ( $p < 0.05$ ), followed by 2.4-fold higher in perithecia and lowest expression during the infective stages, as shown in Fig 3, during appressorium development (8 hpi) and *in planta* growth (48 hpi).

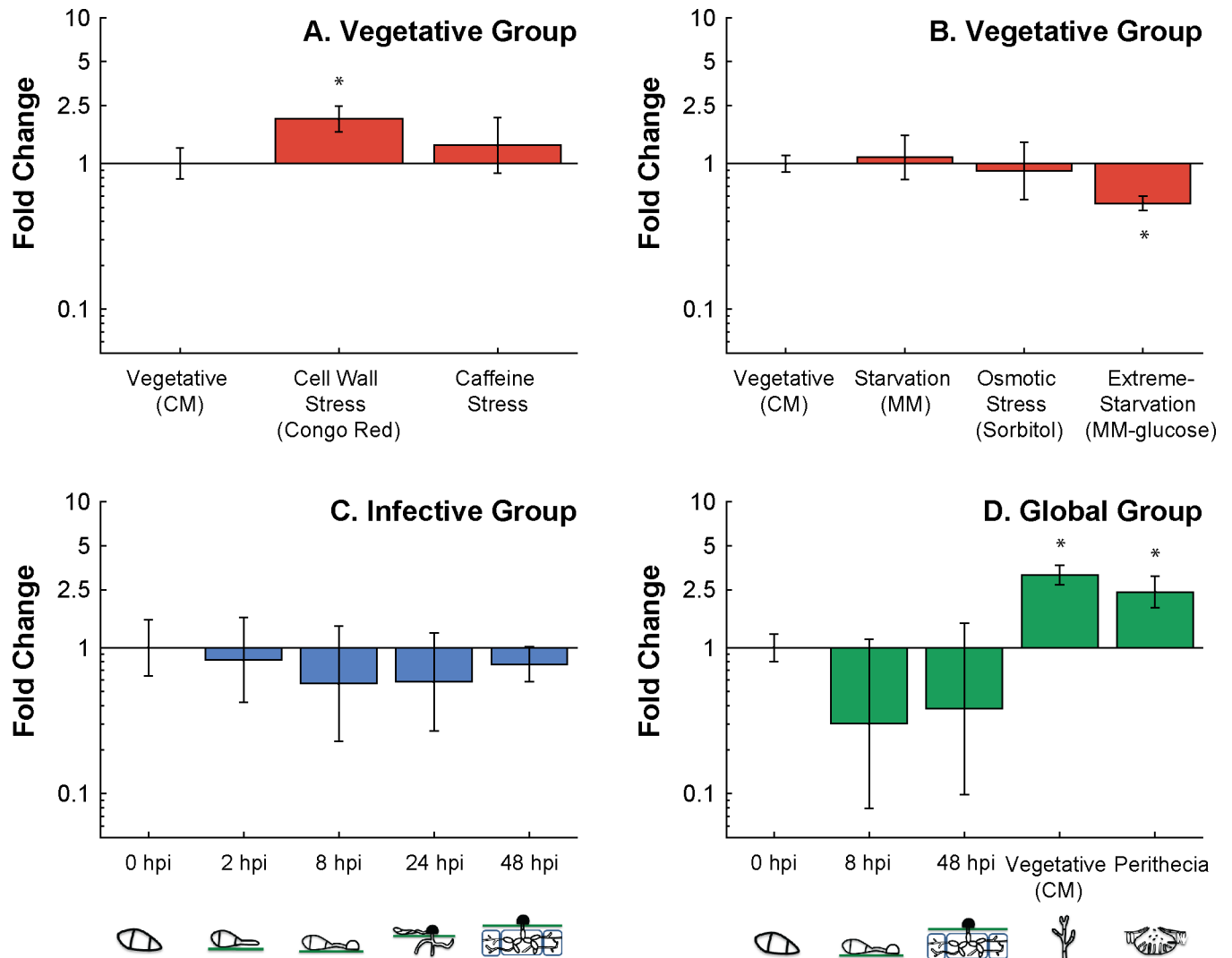


**Fig 3. The expression profile of *M. oryzae* *MGG\_Crh2* cell wall remodelling gene measured by qRT-PCR.** A total of 12 different tissue samples were assigned into three distinct tissue groups: Vegetative, Infective, and Global group each containing 5–6 tissue types. Each graph was assayed and analysed separately. Each bar corresponds to three biological replicates of the same tissue. Error bars are at 95% confidence interval. Panel A. Vegetative group. The expression of *MGG\_Crh2* when vegetatively grown under cell wall stress induced by Congo Red (100 µg/mL) and caffeine (25 mM) relative to growth under optimal conditions in CM. Reference genes *MGG\_Ef1* and *MGG\_40s* were used as the normalising factor. Panel B. Vegetative group. The expression of *MGG\_Crh2* when vegetatively grown under starvation (MM), osmotic stress (Sorbitol 1M) and extreme starvation (MM-glucose), relative to growth under optimal conditions (CM). Reference genes *MGG\_Ef1* and *MGG\_40s* were used as the normalising factor. Panel C. Infective Group. The expression of *MGG\_Crh2* at 2 hpi (germ tube), 8 hpi (immature appressorium), 24 hpi (penetration and early invasive growth), and 48 hpi (*in-planta*) relative to 0 hpi (dormant spores). Reference genes *MGG\_Actin* and *MGG\_40s* were used as the normalising factor. Panel D. Global group. The expression of *MGG\_Crh2* at 8 hpi (immature appressorium), 48 hpi (*in-planta*), vegetative mycelium (CM) and in perithecia, relative to dormant spores (0 hpi). Reference genes *MGG\_Ef1* and *MGG\_40s* were used as the normalising factor.

doi:10.1371/journal.pone.0160637.g003

In summary, this expression study has shed light into the regulatory profile of the transglycosylase cell wall remodelling gene, *MGG\_Crh2*, which was found to be most highly expressed during vegetative growth with down-regulation during the development of infective structures and *in planta* growth. We also have identified an optimum set of control genes for studying gene expression across the life-cycle of *M. oryzae* using qRT-PCR. Further work is required to expand this gene-set to cover a broader range of growth conditions, such as varied exogenous



stresses, but this robust approach sets a standard of practice for qRT-PCR gene analysis which can only increase our understanding of this devastating rice pathogen.

## Supporting Information

### **S1 Dataset. Data analysis for the expression profile of *MGG\_Crh2*.**

(XLSX)

**S1 Fig. Primer specificity analysis by PCR and subsequent size separation by gel electrophoresis for each targeted gene.** Products were PCR amplified using pooled cDNA template from all samples and size separated alongside GeneRuler Ultra Low Range DNA Ladder (10–300 bp). Gel electrophoresis was conducted in 2% agarose (SIGMA-Aldrich).

(TIF)

**S2 Fig. Primer specificity analysis by melt-curve graphs for each targeted gene.** Graphs show PCR product dissociation curves for ten primer pairs used in this analysis using pooled cDNA of WT from all samples used. The melt curve data was obtained from the denaturation of amplified PCR product executed at the end of a qRT-PCR run, by temperature increment.

(TIF)

**S3 Fig. Real-Time PCR primer efficiency analysis.** The cycle threshold (ct) of ten primer pairs for candidate reference genes plotted against a five-fold dilution of pooled cDNA from all samples analysed. Each qRT-PCR reaction had two technical replicates, therefore the cycle threshold (ct) value above is an averaged data. All reactions conducted on the same 96-well plate. The slopes and  $r^2$  values were calculated using a regression line across four-points.

(TIF)

**S4 Fig. Sample RNA quality analysis by electrophoretic separation for samples containing only pathogen RNA.** Each electrophoregram comprise of RNA of fungal tissue grown vegetatively under various conditions, dormant spore (0 hpi) or perithecia. Each graph showed the presence of two sharp peaks, corresponding to two bands on the right side of each graph, indicating good quality RNA.

(TIF)

**S5 Fig. Sample RNA quality analysis by electrophoretic separation for samples containing RNA from both host and pathogen.** Each electrophoregram comprise of RNA taken from host leaf tissue inoculated with fungal spores (in 0.2% gelatine) at various hours post inoculation (hpi). Control leaf comprise of plant leaf sprayed with 0.2% gelatine. Each graph above showed the presence of two sharp peaks, corresponding to two bands on the right side of each graph, indicating undegraded RNA. Additional peaks correspond to chloroplastic ribosomes abundant in samples derived from host leaf tissues.

(TIF)

## Author Contributions

**Conceptualization:** SCO SJG GM.

**Data curation:** SCO MAB.

**Formal analysis:** SCO MAB.

**Funding acquisition:** SJG.

**Investigation:** SCO SJG.

**Methodology:** SCO GM.

**Project administration:** SJG GMP.

**Resources:** SCO.

**Software:** SCO.

**Supervision:** SJG GMP.

**Validation:** SCO.

**Visualization:** SCO MAB.

**Writing – original draft:** SCO SJG.

**Writing – review & editing:** SJG GMP MAB GM.

## References

1. Couch BC, Kohn LM. A multilocus gene genealogy concordant with host preference indicates segregation of a new species, *Magnaporthe oryzae*, from *M. grisea*. *Mycologia*. 2002; 94(4):683–93. PMID: [21156541](#)
2. Mishra D, Singh U, Dash A, Reddy J, Sridhar R, George M, et al. Analysis of *Pyricularia grisea* populations from three different blast epidemics. *International Rice Research Notes*. 2006.
3. Lee FN, Cartwright R, Jia Y, Correll J. Field resistance expressed when the PI-TA gene is compromised by *Magnaporthe oryzae*. *Advances in Genetics, Genomics and Control of Rice Blast Disease*. 2009:281–9.
4. Wilson RA, Talbot NJ. Under pressure: investigating the biology of plant infection by *Magnaporthe oryzae*. *Nature Reviews Microbiology*. 2009; 7(3):185–95. doi: [10.1038/nrmicro2032](#) PMID: [19219052](#)
5. Kasetsoomboon T, Kate-Ngam S, Sriwongchai T, Zhou B, Jantasuriyarat C. Sequence variation of avirulence gene AVR-Pita1 in rice blast fungus, *Magnaporthe oryzae*. *Mycological progress*. 2013; 12(4):617–28.
6. Oerke EC, Dehne HW. Safeguarding production—losses in major crops and the role of crop protection. *Crop Protection*. 2004; 23(4):275–85.
7. Skamnioti P, Gurr SJ. Against the grain: safeguarding rice from rice blast disease. *Trends in biotechnology*. 2009; 27(3):141–50. doi: [10.1016/j.tibtech.2008.12.002](#) PMID: [19187990](#)
8. Fisher MC, Henk DA, Briggs CJ, Brownstein JS, Madoff LC, McCraw SL, et al. Emerging fungal threats to animal, plant and ecosystem health. *Nature*. 2012; 484(7393):186–94. doi: [10.1038/nature10947](#) PMID: [22498624](#)
9. Klis FM, Boorsma A, De Groot P. Cell wall construction in *Saccharomyces cerevisiae*. *Yeast*. 2006; 23(3):185–240. PMID: [16498706](#)
10. Gow NAR, Gadd GM. *The growing fungus*: Springer; 1995.
11. Bowman SM, Free SJ. The structure and synthesis of the fungal cell wall. *Bioessays*. 2006; 28(8):799–808. PMID: [16927300](#)
12. Hurtado-Guerrero R, Schüttelkopf AW, Mouyna I, Ibrahim AF, Shepherd S, Fontaine T, et al. Molecular mechanisms of yeast cell wall glucan remodeling. *Journal of Biological Chemistry*. 2009; 284(13):8461–9. doi: [10.1074/jbc.M807990200](#) PMID: [19097997](#)
13. Calderon J, Zavrel M, Ragni E, Fonzi WA, Rupp S, Popolo L. *PHR1*, a pH-regulated gene of *Candida albicans* encoding a glucan-remodelling enzyme, is required for adhesion and invasion. *Microbiology*. 2010; 156(8):2484–94.
14. Mouyna I, Fontaine T, Vai M, Monod M, Fonzi WA, Diaquin M, et al. Glycosylphosphatidylinositol-anchored glucanoyltransferases play an active role in the biosynthesis of the fungal cell wall. *Journal of Biological Chemistry*. 2000; 275(20):14882–9. PMID: [10809732](#)
15. Pardini G, De Groot PWJ, Coste AT, Karababa M, Klis FM, de Koster CG, et al. The CRH family coding for cell wall GPI proteins with a predicted transglycosidase domain affects cell wall organization and virulence of *Candida albicans*. *Journal of Biological Chemistry*. 2006.
16. Cabib E, Blanco N, Grau C, Rodriguez Pena JM, Arroyo J. Crh1p and Crh2p are required for the cross linking of chitin to (1-6) glucan in the *Saccharomyces cerevisiae* cell wall. *Molecular microbiology*. 2007; 63(3):921–35. PMID: [17302808](#)

17. Kitagaki H, Wu H, Shimoi H, Ito K. Two homologous genes, *DCW1* (*YKL046c*) and *DFG5*, are essential for cell growth and encode glycosylphosphatidylinositol-(GPI)-anchored membrane proteins required for cell wall biogenesis in *Saccharomyces cerevisiae*. *Molecular microbiology*. 2002; 46(4):1011–22. PMID: [12421307](#)
18. Pardo M, Monteoliva L, Vázquez P, Martínez R, Molero G, Nombela C, et al. *PST1* and *ECM33* encode two yeast cell surface GPI proteins important for cell wall integrity. *Microbiology*. 2004; 150(12):4157–70.
19. Rodríguez-Pena JM, Cid VJ, Arroyo J, Nombela C. A novel family of cell wall-related proteins regulated differently during the yeast life cycle. *Molecular and cellular biology*. 2000; 20(9):3245. PMID: [10757808](#)
20. Hwang JS, Seo DH, Kim JY. Soluble forms of YICrh1p and YICrh2p, cell wall proteins of *Yarrowia lipolytica*, have beta-(1,3) glycosidase activity. *Yeast*. 2006; 23(11):803–12. PMID: [16921554](#)
21. Blanco N, Sanz AB, Rodríguez-Peña JM, Nombela C, Farkaš V, Hurtado-Guerrero R, et al. Structural and functional analysis of yeast Crh1 and Crh2 transglycosylases. *FEBS Journal*. 2015.
22. Dague E, Bitar R, Ranchon H, Durand F, Yken HM, Francois JM. An atomic force microscopy analysis of yeast mutants defective in cell wall architecture. *Yeast*. 2010; 27(8):673–84. doi: [10.1002/yea.1801](#) PMID: [20602335](#)
23. Guerriero G, Silvestrini L, Obersiebnig M, Salerno M, Pum D, Strauss J. Sensitivity of *Aspergillus nidulans* to the Cellulose Synthase Inhibitor Dichlobenil: Insights from Wall-Related Genes' Expression and Ultrastructural Hyphal Morphologies. *PLoS One*. 2013; 8(11):e80038. doi: [10.1371/journal.pone.0080038](#) PMID: [24312197](#)
24. Alberti-Segui C, Morales AJ, Xing H, Kessler MM, Willins DA, Weinstock KG, et al. Identification of potential cell surface proteins in *Candida albicans* and investigation of the role of a putative cell surface glycosidase in adhesion and virulence. *Yeast*. 2004; 21(4):285–302. PMID: [15042589](#)
25. Boorsma A, Nobel Hd, Riet Bt, Bargmann B, Brul S, Hellingwerf KJ, et al. Characterization of the transcriptional response to cell wall stress in *Saccharomyces cerevisiae*. *Yeast*. 2004; 21(5):413–27. PMID: [15116342](#)
26. Garcia R, Bermejo C, Grau C, Perez R, Rodríguez-Pena JM, Francois J, et al. The global transcriptional response to transient cell wall damage in *Saccharomyces cerevisiae* and its regulation by the cell integrity signaling pathway. *Journal of Biological Chemistry*. 2004; 279(15):15183–95. PMID: [14739279](#)
27. Park S-Y, Choi J, Lim S-E, Lee G-W, Park J, Kim Y, et al. Global Expression Profiling of Transcription Factor Genes Provides New Insights into Pathogenicity and Stress Responses in the Rice Blast Fungus. *PLoS pathogens*. 2013; 9(6):e1003350. doi: [10.1371/journal.ppat.1003350](#) PMID: [23762023](#)
28. Kawahara Y, Oono Y, Kanamori H, Matsumoto T, Itoh T, Minami E. Simultaneous RNA-Seq analysis of a mixed transcriptome of rice and Blast fungus interaction. *PLoS one*. 2012; 7(11):e49423. doi: [10.1371/journal.pone.0049423](#) PMID: [23139845](#)
29. Bustin S. Quantification of mRNA using real-time reverse transcription PCR (RT-PCR): trends and problems. *Journal of molecular endocrinology*. 2002; 29(1):23–39. PMID: [12200227](#)
30. Broad Institute of Harvard and MIT. Magnaporthe comparative Sequencing Project 2011. Available from: <http://www.broadinstitute.org/>.
31. Czechowski T, Bari RP, Stitt M, Scheible WÄd, Udvardi MK. Real-time RT-PCR profiling of over 1400 *Arabidopsis* transcription factors: unprecedented sensitivity reveals novel root-and shoot-specific genes. *The Plant Journal*. 2004; 38(2):366–79. PMID: [15078338](#)
32. Guenin S, Mauriat M, Pelloux J, Van Wuytswinkel O, Bellini C, Gutierrez L. Normalization of qRT-PCR data: the necessity of adopting a systematic, experimental conditions-specific, validation of references. *Journal of experimental botany*. 2009; 60(2):487–93. doi: [10.1093/jxb/ern305](#) PMID: [19264760](#)
33. Gutierrez L, Mauriat M, Guenin S, Pelloux J, Lefebvre JF, Louvet R, et al. The lack of a systematic validation of reference genes: a serious pitfall undervalued in reverse transcription, Åpolymerase chain reaction (RT, ÅPCR) analysis in plants. *Plant biotechnology journal*. 2008; 6(6):609–18. doi: [10.1111/j.1467-7652.2008.00346.x](#) PMID: [18433420](#)
34. Bustin SA, Benes V, Garson JA, Hellems J, Huggett J, Kubista M, et al. The MIQE guidelines: minimum information for publication of quantitative real-time PCR experiments. *Clinical chemistry*. 2009; 55(4):611–22. doi: [10.1373/clinchem.2008.112797](#) PMID: [19246619](#)
35. Dheda K, Huggett J, Chang J, Kim L, Bustin S, Johnson M, et al. The implications of using an inappropriate reference gene for real-time reverse transcription PCR data normalization. *Analytical biochemistry*. 2005; 344(1):141–3. PMID: [16054107](#)
36. Thellin O, Zorzi W, Lakaye B, De Borman B, Coumans B, Hennen G, et al. Housekeeping genes as internal standards: use and limits. *Journal of biotechnology*. 1999; 75(2):291–5.

37. Schmittgen TD, Livak KJ. Analyzing real-time PCR data by the comparative CT method. *Nature protocols*. 2008; 3(6):1101–8. PMID: [18546601](#)
38. Ling D, Salvaterra PM. Robust RT-qPCR data normalization: validation and selection of internal reference genes during post-experimental data analysis. *PLoS one*. 2011; 6(3):e17762. doi: [10.1371/journal.pone.0017762](#) PMID: [21423626](#)
39. Scholtz JJ, Visser B. Reference gene selection for qPCR gene expression analysis of rust-infected wheat. *Physiological and molecular plant pathology*. 2013; 81:22–5.
40. Kim H-K, Yun S-H. Evaluation of potential reference genes for quantitative RT-PCR analysis in *Fusarium graminearum* under different culture conditions. *The Plant Pathology Journal*. 2011; 27(4):301–9.
41. Bohle K, Jungebloud A, Gocke Y, Dalpiaz A, Cordes C, Horn H, et al. Selection of reference genes for normalisation of specific gene quantification data of *Aspergillus niger*. *Journal of biotechnology*. 2007; 132(4):353–8. PMID: [17868942](#)
42. Chen J, Zheng W, Zheng S, Zhang D, Sang W, Chen X, et al. Rac1 is required for pathogenicity and Chm1-dependent conidiogenesis in rice fungal pathogen *Magnaporthe grisea*. *PLoS pathogens*. 2008; 4(11):e1000202. doi: [10.1371/journal.ppat.1000202](#) PMID: [19008945](#)
43. Yan X, Ma W-B, Li Y, Wang H, Que Y-W, Ma Z-H, et al. A sterol 14- $\alpha$ -demethylase is required for conidiation, virulence and for mediating sensitivity to sterol demethylation inhibitors by the rice blast fungus *Magnaporthe oryzae*. *Fungal Genetics and Biology*. 2011; 48(2):144–53.
44. Raman V, Simon SA, Romag A, Demirci F, Mathioni SM, Zhai J, et al. Physiological stressors and invasive plant infections alter the small RNA transcriptome of the rice blast fungus, *Magnaporthe oryzae*. *BMC genomics*. 2013; 14(1):326.
45. Talbot NJ, Ebbole DJ, Hamer JE. Identification and characterization of *MPG1*, a gene involved in pathogenicity from the rice blast fungus *Magnaporthe grisea*. *The Plant Cell Online*. 1993; 5(11):1575–90.
46. Oh Y, Donofrio N, Pan H, Coughlan S, Brown DE, Meng S, et al. Transcriptome analysis reveals new insight into appressorium formation and function in the rice blast fungus *Magnaporthe oryzae*. *Genome Biol*. 2008; 9(5):R85. doi: [10.1186/gb-2008-9-5-r85](#) PMID: [18492280](#)
47. Haiyan H, Jieyun Z, Kangle Z, Mingjiu L. Characterization of differentially expressed genes induced by virulent and avirulent *Magnaporthe grisea* strains in rice. *Plant Omics*. 2012; 5(6):542–6.
48. Mathioni S, Beló A, Rizzo CJ, Dean RA, Donofrio NM. Transcriptome profiling of the rice blast fungus during invasive plant infection and in vitro stresses. *BMC Genomics*. 2011; 12(1):49.
49. Soanes DM, Chakrabarti A, Paszkiewicz KH, Dawe AL, Talbot NJ. Genome-wide transcriptional profiling of appressorium development by the rice blast fungus *Magnaporthe oryzae*. *PLoS pathogens*. 2012; 8(2):e1002514. doi: [10.1371/journal.ppat.1002514](#) PMID: [22346750](#)
50. Skamnioti P, Gurr SJ. *Magnaporthe grisea* cutinase2 mediates appressorium differentiation and host penetration and is required for full virulence. *The Plant Cell Online*. 2007; 19(8):2674.
51. Hellemans J, Mortier G, De Paepe A, Speleman F, Vandesompele J. qBase relative quantification framework and software for management and automated analysis of real-time quantitative PCR data. *Genome biology*. 2007; 8(2):R19. PMID: [17291332](#)
52. Pfaffl MW. A new mathematical model for relative quantification in real-time RT-PCR. *Nucleic acids research*. 2001; 29(9):e45. PMID: [11328886](#)
53. Vandesompele J, De Preter K, Pattyn F, Poppe B, Van Roy N, De Paepe A, et al. Accurate normalization of real-time quantitative RT-PCR data by geometric averaging of multiple internal control genes. *Genome biology*. 2002; 3(7):research0034. PMID: [12184808](#)
54. Cherry JM, Hong EL, Amundsen C, Balakrishnan R, Binkley G, Chan ET, et al. *Saccharomyces Genome Database: the genomics resource of budding yeast*. *Nucleic acids research*. 2011; gkr1029.
55. Altschul SF, Gish W, Miller W, Myers EW, Lipman DJ. Basic local alignment search tool. *Journal of molecular biology*. 1990; 215(3):403–10. PMID: [2231712](#)
56. Krupp G. Stringent RNA quality control using the Agilent 2100 bioanalyzer. In: Agilent Technologies I, editor. *Agilent Technologies Application Notes*. United States of America 2005.
57. Babu S, Gassmann M. Assessing integrity of plant RNA with the Agilent 2100 Bioanalyzer. In: Agilent Technologies I, editor. *Agilent Technologies Application Notes*. United States of America 2011.
58. Sandbaken MG, Culbertson MR. Mutations in elongation factor EF-1  $\alpha$  affect the frequency of frameshifting and amino acid misincorporation in *Saccharomyces cerevisiae*. *Genetics*. 1988; 120(4):923–34. PMID: [3066688](#)
59. Planta RJ, Mager WH. The list of cytoplasmic ribosomal proteins of *Saccharomyces cerevisiae*. *Yeast*. 1998; 14(5):471–7. PMID: [9559554](#)

60. Kuranda K, Leberre V, Sokol S, Palamarczyk G, François J. Investigating the caffeine effects in the yeast *Saccharomyces cerevisiae* brings new insights into the connection between TOR, PKC and Ras/cAMP signalling pathways. *Molecular Microbiology*. 2006; 61(5):1147–66. PMID: [16925551](#)
61. Mehrabi R, Ding S, Xu J-R. MADS-box transcription factor Mig1 is required for infectious growth in *Magnaporthe grisea*. *Eukaryotic Cell*. 2008; 7(5):791–9. doi: [10.1128/EC.00009-08](#) PMID: [18344407](#)
62. Kong LA, Yang J, Li G, Qi LL, Zhang YJ, Wang CF, et al. Different chitin synthase genes are required for various developmental and plant infection processes in the rice blast fungus *Magnaporthe oryzae*. *Plos Pathogens*. 2012; 8(2):e1002526. doi: [10.1371/journal.ppat.1002526](#) PMID: [22346755](#)
63. Franck WL, Gokce E, Oh Y, Muddiman DC, Dean RA. Temporal analysis of the *Magnaporthe oryzae* proteome during conidial germination and cyclic AMP (cAMP)-mediated appressorium formation. *Molecular & Cellular Proteomics*. 2013; 12(8):2249–65.
64. Zelante T, Iannitti RG, De Luca A, Arroyo J, Blanco N, Servillo G, et al. Sensing of mammalian IL-17A regulates fungal adaptation and virulence. *Nature communications*. 2012; 3:683. doi: [10.1038/ncomms1685](#) PMID: [22353714](#)
65. Stuehler C, Khanna N, Bozza S, Zelante T, Moretti S, Kruhm M, et al. Cross-protective TH1 immunity against *Aspergillus fumigatus* and *Candida albicans*. *Blood*. 2011; 117(22):5881. doi: [10.1182/blood-2010-12-325084](#) PMID: [21441461](#)
66. Arroyo J, Sarfati J, Baixench MT, Ragni E, Guillen M, Rodriguez Pena JM, et al. The GPI anchored Gas and Crh families are fungal antigens. *Yeast*. 2007; 24(4):289–96. PMID: [17397107](#)
67. Jolink H, Meijssen IC, Hagedoorn RS, Arentshorst M, Drijfhout JW, Mulder A, et al. Characterization of the T-Cell-Mediated Immune Response Against the *Aspergillus fumigatus* Proteins Crf1 and Catalase 1 in Healthy Individuals. *Journal of Infectious Diseases*. 2013; 208(5):847–56. doi: [10.1093/infdis/jit237](#) PMID: [23698813](#)
68. Fujikawa T, Kuga Y, Yano S, Yoshimi A, Tachiki T, Abe K, et al. Dynamics of cell wall components of *Magnaporthe grisea* during infectious structure development. *Molecular microbiology*. 2009; 73(4):553–70. doi: [10.1111/j.1365-2958.2009.06786.x](#) PMID: [19602150](#)